PROCEEDINGS, 44th Workshop on Geothermal Reservoir Engineering
Stanford University, Stanford, California, February 11-13, 2019
SGP-TR-214

Demonstration Tests of a Robust Engineered Geothermal System

G. Danko[1,2], A. Jobbik[2], M. K. Baracza[2], G. Varga[2], I. Kovacs[3], and V. Wittig[4]

1. University of Nevada, Reno, Reno, 1664 Virginia Str, Reno, NV, 89557, USA, danko@unr.edu

2. Research Institute of Applied Earth Sciences, University of Miskolc, Hungary

3. EU-FIRE Ltd., Hungary

4.GZB, Germany

Keywords: Robust EGS, hydrofracture, wing fracture, single-well geothermal arrangement

ABSTRACT

Geothermal energy generation from hot dry rock is far beyond its potential in the U.S. and the world. EGS is the most promising energy source yet the least successful amongst all renewable energy forms. There are many reasons: (1) high risks from largely unknown geologic variables; (2) faults in the design concepts of currently used solutions relying on fracture opening partially by fluid pressure, making the joint's aperture an operational variable and thus inherently projecting seismic activities with changing pressures and temperatures; (3) inherent loss of coolant water and energy due to excessive injection pressures as a consequence of the faulty concept, abysmal fracture aperture, and consequent large circulation loss in the currently known EGS solutions.

A new, robust EGS (REGS) technology tryout is underway with innovative fracture permeability creation and control. The geometry, aperture support technique and coolant fluid flow isolation system are all robustly planned and created according to an invention. The new elements of the REGS technology are step-by-step tested and demonstrated in an international research cooperation with researchers from the USA and the EU. Planning for small-field-scale, directional drilling and fracturing experiments are underway to achieve a planar wing fracture or fractures osculating along the well trajectory at shallow depth. Laboratory-scale, hardening grouting injection experiments are built to demonstrate the creation of a central support island in each planar wing fracture. Numerical models are developed to scale the experimental results for the field-scale design of the REGS. Small-scale, experimental studies of Well-Fracture-Well fluid circulation experiments are used to verify the numerical model results for upscaling. Predicted scenarios are studied with scaled numerical models for full-scale REGS applications for wide-scale applications in (a) electrical power generation; and (b) heating use in communal or industrial examples.

The tests are expected to prove the key components of the REGS geologic heat exchanger with stabilized, large fracture aperture and controlled flow zones for minimized opening pressure loss, seismicity and maximized energy extraction. The key to energy extraction is the zonal isolation of fracture flow by a grouted, blocking island between injection and extraction points of any planar fracture, forcing the coolant fluid away of the island to sweep large surface area of the planar fracture for heat exchange. The key to the creation of a series of large, planar, wing fractures is a directionally-drilled well to follow each planar fracture, intersecting it at multiple points around a section at which the fracture approximates the osculating plane of the well. The key of the robustness is the step-by-step construction of a REGS with: directional drilling; wing-type fracturing; testing for connectivity of each planar, wing fracture with the well; continuation of the construction and testing of a series of wing fractures along the directional drilled well whereas the well direction is continuously adjusted (if needed) to the planar directions of the fractures; and completion of the series of wing fractures with zonal insulation in each planar fracture by implanting (injecting) a grouted, blocking island between the injection and extraction sections of the well connections to each wing fracture.

The paper reports the new results from the laboratory-scale REGS tests and their numerical scaling models; as well as the design of the field-scale experiments in a well drilled in hot, dry rock.

1. INTRODUCTION

Geothermal energy generation from hot dry rock is far beyond its potential in the U.S. and the world. EGS is the most promising energy source yet the least successful amongst all renewable energy forms (DOE, 2006). There are many reasons: (1) high risks from largely unknown geologic variables; (2) faults in the design concepts of currently used solutions relying on fracture opening partially by fluid pressure, making the joint's aperture an operational variable and thus inherently projecting seismic activities with changing pressures and temperatures; (3) inherent loss of coolant water and energy due to excessive injection pressures as a consequence of the faulty concept, abysmal fracture aperture, and consequent large circulation loss in the currently known EGS solutions (Kumar and Ghassemi, 2016, Jung, 2013).

A technology tryout is underway to prove the innovative fracture permeability creation and control. The geometry, aperture support technique and coolant fluid flow isolation system are all robustly planned and created according to an invention (UNR, 2018, Danko et al., 2018). The key of the robustness is the step-by-step construction of a REGS with: directional drilling; wing-type fracturing; testing for connectivity of each planar, wing fracture with the well; continuation of the construction and testing of a series of wing fractures along the directional drilled well whereas the well direction is continuously adjusted (if needed) to the planar directions of the fractures; and completion of the series of wing fractures with zonal insolation in each planar fracture by the injection of a grouted, blocking island

between the intake and the extraction points of the wing fracture section. The key to the creation of a series of large, planar, wing fractures is a directionally-drilled well to follow each planar fracture, intersecting it at multiple points around a section at which the fracture approximates the osculating plane of the well, shown in Figs. 1 and 2.

Subsection headings should be capitalized on the first letter. Avoid using subsections deeper than subsubsections.

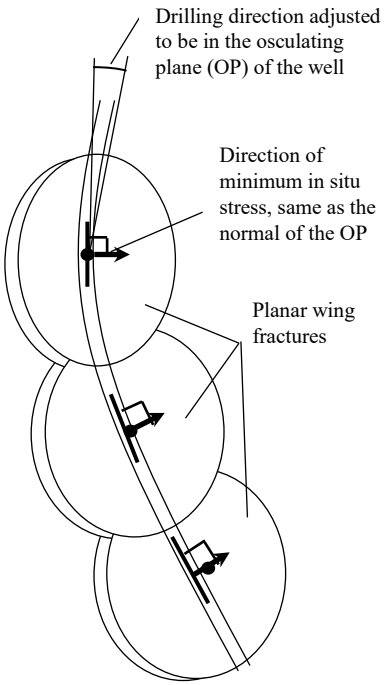

Figure 1: Wing fractures along a main well.

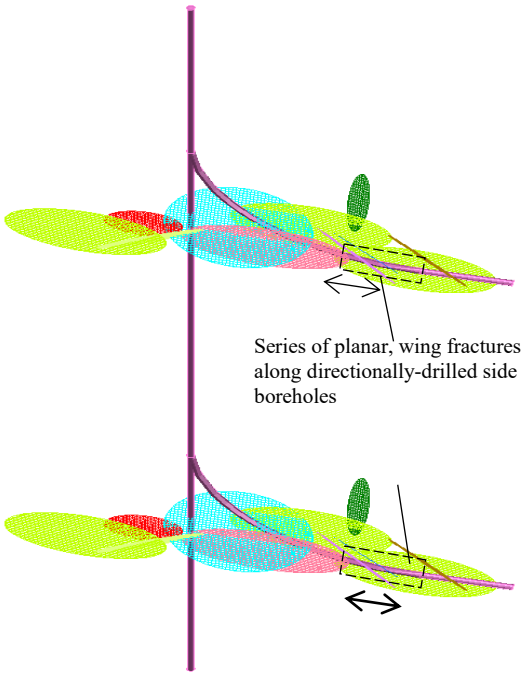

Figure 2: Planar wing fractures along deviated boreholes.

The new elements of the REGS technology are step-by-step tested and demonstrated in an international research cooperation with researchers from the USA and the EU (UNR, 2018). Planning for small-field-scale, directional drilling and fracturing experiments are underway to achieve a planar wing fracture or fractures osculating along the well trajectory at shallow depth. Laboratory-scale, hardening grouting injection experiments are prepared to demonstrate the creation of a central support island in each planar wing fracture. Numerical models are developed to scale the experimental results for the field-scale design of the REGS. Small-scale, experimental studies of Well-Fracture-Well fluid circulation experiments are underway to verify the numerical model results for upscaling. Predicted scenarios are studied with scaled numerical models for full-scale REGS applications for wide-scale applications in electrical power generation and heating in communal or industrial examples.

The tests are expected to prove the key components of the REGS geologic heat exchanger with stabilized, large fracture aperture and controlled flow zones for minimized opening pressure loss, seismicity and maximized energy extraction. The key to energy extraction is seen in creating zonal isolation of fracture flow by a grouted, blocking island between injection and extraction points of any planar fracture, forcing the coolant fluid away of the island to sweep large surface area of the planar fracture for heat exchange.

The paper reports preliminary results from laboratory-scale REGS tests and from a numerical simulation model of a conceptual, single-fracture REGS arrangement. The model results may be used in the design of a field-scale experiment in a well drilled in hot, dry rock.

2. LABORATORY-SCALE TESTS OF THE PHYSICAL MODEL OF REGS

Laboratory-scale tests of certain elements of the REGS arrangement are conducted to move the concept closer to practical applications. Although much work has been conducted on wing fractures and their applications (Cornet, 2016, Zhou et al., 2016), their application in the REGS arrangement needs experimental studies. There are many obstacles in creating a new system at the first time. Some critical elements are related to site characterization, directional drilling, and monitoring tasks, such as (1) drilling into the direction of an unknown fracture plane to be the osculating plain of the drilling section; (2) tryout fracturing for directional accuracy during drilling; and (3) assessing the quality of flow connection between the well and its wing fractures during construction.

Challenges (1) through (3) are the tasks of drilling and fracturing experts and are considered solvable with technology developments driven by the oil and gas industry. There are specific challenges for REGS development, falling outside of the current, mainstream tasks of drilling for oil and gas. Such challenges are: (4) the completion of the planar fractures with the delivery of the grout into the desired area in the center of each planar fracture; and (5) reconnect the flow paths between the un-grouted fracture volumes and the well for coolant fluid injection and extraction for energy production from large heat transport surfaces. Further challenges are (6) the cost and

financial feasibility of creating the REGS arrangement; and (7) to find the optimum order of tasks (1) through (5) for the successful construction of the new REGS arrangement.

Preliminary grouting experiments are conducted in small-scale laboratory settings, emulating the opening of the fracture walls of the rock with two elastic plates as membranes. The goal of the experiments is to explore the controllability of the shape of the grouting island in vertical and inclined fractures. In one experiment, a stainless steel plate of 0.87 m × 1.07 m in size, 1.8 mm in thickness and a plywood plate of 12 mm thick, shown side-by-side in Fig.3, are fastened together along their edges. The plywood plate is connected to injection and extraction ports as well as to pressure monitoring pipes, shown in Fig. 4 for the horizontal fracture experiment. The plates are covered with geotextile to emulate the roughness of the fracture wall.

The deflection of the plates under pressure load across the diameter is determined from the stretched membrane's equation (Hermida, 1991). The fracture profile of opening due to the deflection of each side is calculated to be 12 mm in the center location under 0.2 bar hydrostatic pressure. This value is in excellent agreement with the thickness of the hardened grout island in the center point form the experiment. The deflection profile of the stainless steel plate is shown in Fig. 5.

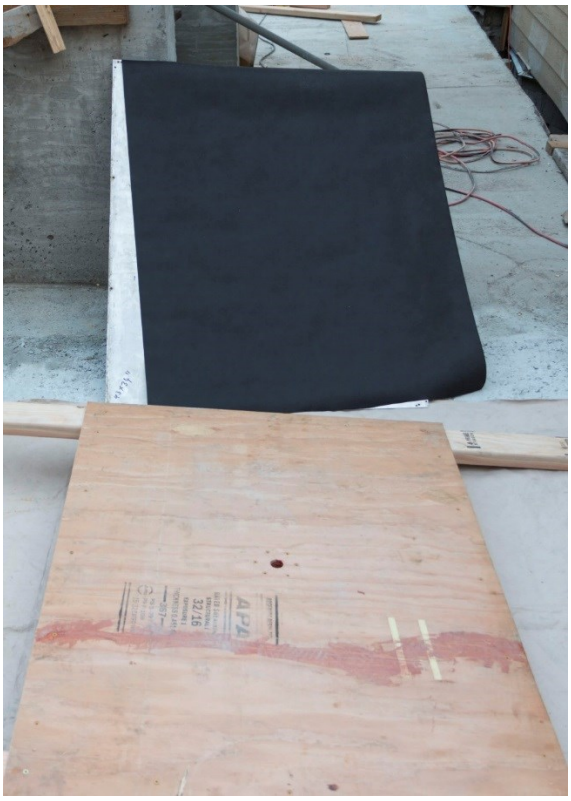

Figure 3: The membrane plates for emulating fracture walls.

Figure 4: The horizontal fracture grouting assembly.

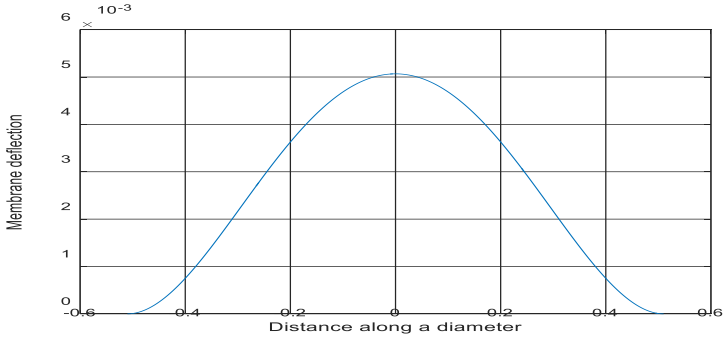

Figure 5: Deflection profile of the stainless steel plate.

Injection of fast-setting water-cement grout in the horizontal assembly was performed under gravitational pressure through the central standpipe, shown in Fig. 4. The shape of the hardened, grouted island was found symmetrical and in the expected thickness from the membrane equation model. Based on the preliminary experiments, it is straightforward to control the size of grouted island by the volume and the viscosity of the mixture in a horizontal fracture.

More careful injection engineering is expected to achieve a grouted island in the center of a vertical fracture. The vertical, stretched membrane assembly is shown in Fig. 6. Several, common-sense ways have been explored to overcome the gravitation force that attracts the injected grout downward. One result is shown in Fig. 7, depicting a close-to-symmetrical grouted island shape, proving the possibility of achieving a desired shape by fluid and slurry flow engineering. Fig. 8 shows the disassembled fracture walls and the attached grouting island.

More detailed, further laboratory experimental studies are underway in fluid flow and grouting injections at the University of Miskolc with an improved stretched membrane assembly, shown in Figs. 9 and 10 in horizontal and vertical positions, respectively.

Figure 6: The vertical fracture grouting assembly.

Figure 7: The grouted island still attached to the separated wall.

Figure 8: The membrane walls of the grouting assembly.

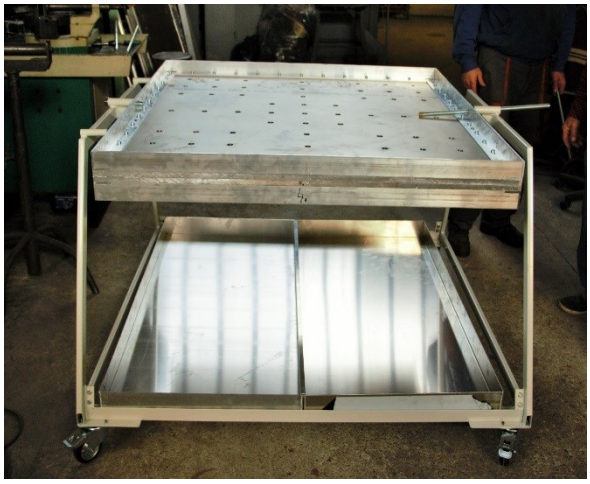

Figure 9: The improved grouting assembly in horizontal position.

3. FIELD--SCALE PLANS FOR THERMAL ENERGY RECOVERY WITH REGS

The REGS arrangement still remains a concept and a hypothesis until it is tried out in the field. However, any field test of the technology requiring deep drilling and hydrofracturing is expensive and unattractive due to risks unless there is an overwhelming advantage for large-scale applications with potential financial gains. A preliminary, cost-benefit study is needed for the feasibility of a REGS field test. Such a concept is described here to test a simplified REGS arrangement for the extraction of thermal energy from deep, dry, exploited oil wells, available by the hundreds, for communal or district heating. The schematic geometry of a dry well is shown in Fig. 11.

Figure 10: The improved membrane assembly in vertical position.

The simplified REGS for Dry Well application is created in four steps as follows:

Step 1. The open, bottom section of the well is hydrofractured through a trammy pipe that is sealed and pressurized, illustrated in Fig.12. It is assumed that the minimum principal stress field direction is horizontal, resulting in a vertical planar fracture, intersecting the vertical well along its full length, parallel with its axis. If this assumption is not proven by the data in the field, the Dry Well may be skipped from the plan; or a correction drilling along the actual fracture plain may be necessary for the open well section.

Step 2. The middle area of the vertical, planar fracture is grouted through a grouting trammy pipe starting from bottom and moving the grout injection gradually upward. A short section is sealed on the lowest point to prevent grouting the bottom area of the planar fracture. The desired geometry of the grouted island in the fracture is shown in Fig. 13.

Step 3. The middle area of the grouted planar fracture and the bottom seal are drilled through to the bottom of the well for accepting the coolant extraction pipe. After drilling, a circulation test is needed for assurance of hydraulic connection between the fracture void space and two sections of the well for injection and extraction. The test and mini-fracturing may be performed through the drill rod. The desired geometry of the coolant extraction pipe and the coolant fluid circulation system are shown in Fig. 14.

Step 4. The production pipe is inserted from the surface to the bottom of the well for coolant fluid recovery for geothermal energy extraction. The coolant extraction pipe is thermally-coated along its entire length and it is sealed through the grouted section after insertion.

The conceptual arrangement is used in the engineering model for quantifying the expected thermal energy capacity of a single-well arrangement. The input data for two cases (Case 1 and Case 2) are given in Table 1.

Table 1. Input data for Dry Wells.

Property	Case 1	Case 2	Unit
Flow rate	15	15	kg/s
Injection water temperature	40	40	^oC
Depth of lined well	2000	2000	m
Planar fracture diameter	600	600	m
Rock thermal conductivity	3.5	1.28	W/(mK)
Specific heat	930	930	J/(kgK)
Density of the rock	2700	1980	kg/m^3
Rock temperature at surface	10	10	^oC
Rock thermal gradient	0.05	0.05	$^oC/m$

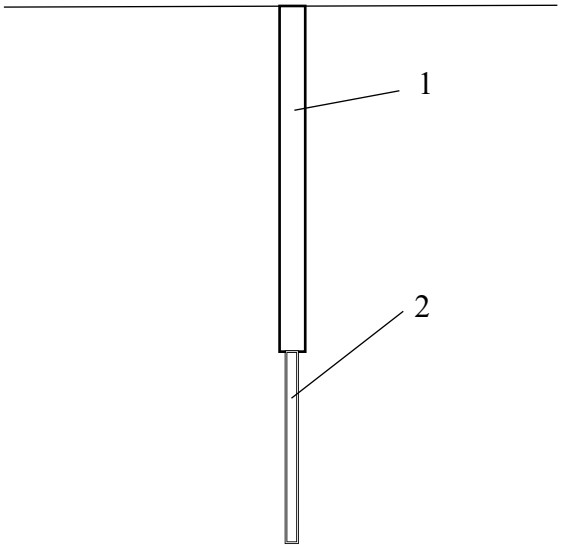

Figure 11: The Dry Well (1 Lined Well Section, 2,000 m, 7" diameter; 2 Open Well Section, 600 m, 6" diameter).

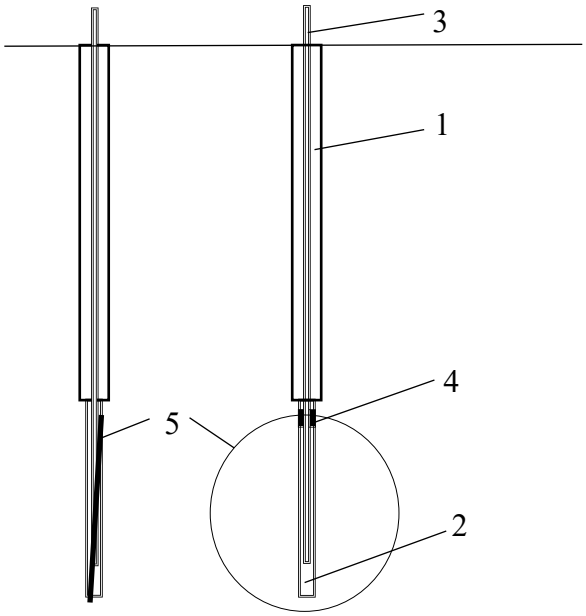

Figure 12: Hydrofracturing the Dry Well (1 Lined Well Section; 2 Open Well Section; 3 Fracturing trammy pipe; 4 Pressure Seal; 5 Planar fracture in plain view and in side view).

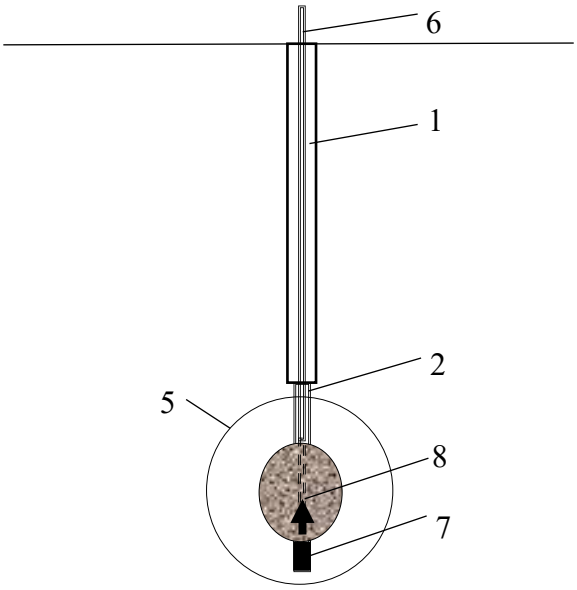

Figure 13: Grouting the Dry Well (1 Lined Well Section; 2 Open Well Section; 5 Planar fracture in plain view; 6 Grouting trammy pipe; 7 Bottom Seal; 8 Grouting trummy pipe moving direction).

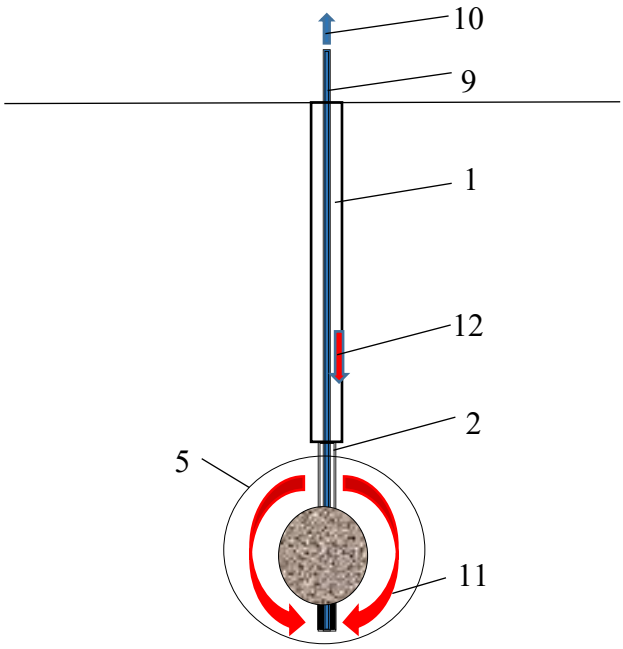

Figure 14: Drilling and inserting the coolant collection pipe in the Dry Well (1 Lined Well Section; 2 Open Well Section; 5 Planar fracture in plain view; 9 Coolant collection pipe; 10 Heated fluid; 11 Coolant-to-heated flow pattern in planar fracture; 12 Coolant injection fluid).

4. MATHEMATICAL MODEL OF REGS FOR ENERGY RECOVERY

The geothermal module of the MULTIFLUX flow and thermal simulation code (Danko, 2008, Bahrami et al., 2016) is used in the preliminary study to predict the expected thermal energy capacity of a single-fracture Dry Well REGS arrangement. The coupled, T-H-M-C network model in MULTIFLUX is reduced for the present study to using only the T-H model parts whereas the mechanical model part is replaced with a fixed-aperture model, assuming a pre-defined, near-lens-shaped fracture cross section. The goal of the model simulation is to quantify the thermal capacity and thermal drawdown for a 30-year time period for Cases 1 and 2.

4.1 The Input Parameters for the Hydraulic and Thermal Models

The main input parameters for the single-fracture, single-well model match those given in Section 4 and in Table 1. Furthermore, the maximum fracture aperture at the center of the fracture is fixed at 0.015 m, tapered down to zero toward the edge of the planar fracture. This large aperture is made possible by the one-time fracture opening via a grout-injecting pressure overcoming the minimum principal stress in the rock strata.

The coolant fluid passes down in the annulus between the well's liner and the returning pipe, assumed to be 0.075 m (3") in outside diameter, increased by thermal insulation of 0.02 m in thickness and 0.2 W/(mK) in thermal conductivity, a moderate value, assuming to be of a low-density, high-strength plastic coating of the 3" pipe. The thermal model of the downhole well includes heat convection between the downward coolant fluid and the well liner; and transient heat conduction in the rock around the well, cooling (or heating) the well from the outside. In the inside of the well, heat convection is modeled between the 3" pipe and the coolant fluid; heat conduction considered through the thermal insulation and the pipe's wall; heat convection included inside the 3" pipe between its wall and the upcoming hot coolant fluid; as well as heat advection is modeled inside the upstream flow.

The flow field in the planar fracture is assumed to be divided into three paths (Path 1, Path 2 and Path 3), discretized into pixels, shown in Fig.15. The length, width and surface area of each pixel are depicted along each path in Figs. 16, 17, and 18, respectively. The total fluid flow is divided into these three paths as an input to the model, affected by the hydraulic resistances of the paths. Since no field data may be obtained for the split, nor active flow control is planned, sensitivity to the split of the total flow rate to pats is evaluated. An optimum distribution may be uniquely determined by matching a common exit temperatures for Path 1, Path 2 and Path 3, maximizing thermal performance. The optimized flow rate splits between Path 1, Path 2 and Path 3 are found to be 47%, 28%, and 25%, respectively for the example. Thermal connections between the pixels are accounted for by advection, conduction and convection. Thermal connections between the pixels and the rock strata include heat convection on the fracture surface; and transient heat conduction in the rock strata toward the undisturbed, virgin rock temperature that is a function of elevation. A more realistic flow rate distribution may be expected as 20%, 35%, and 45% for Path 1, Path 2 and Path 3 in a lens-shaped planar fracture, due to an increasing fracture aperture and decreasing path length toward the center support island. Such split is also modeled for comparison with the optimum flow distribution.

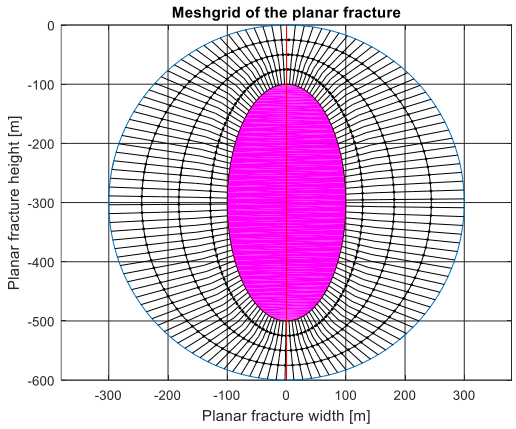

Figure 15: Discretized fracture with pixels.

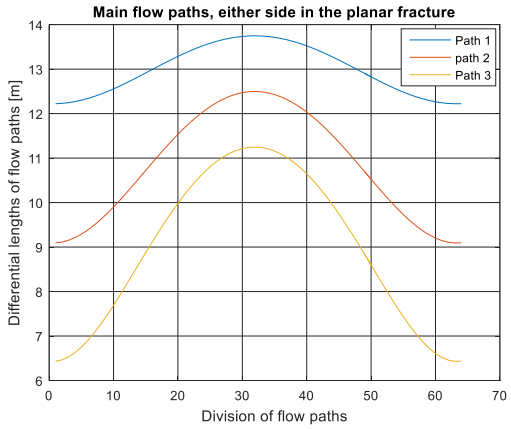

Figure 16: The length of each pixel along the flow path.

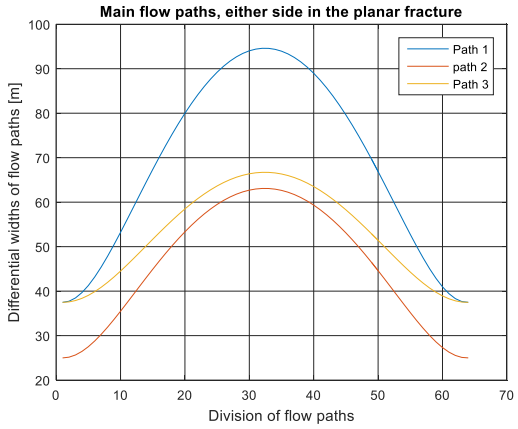

Figure 17: The width of each pixel along the flow path.

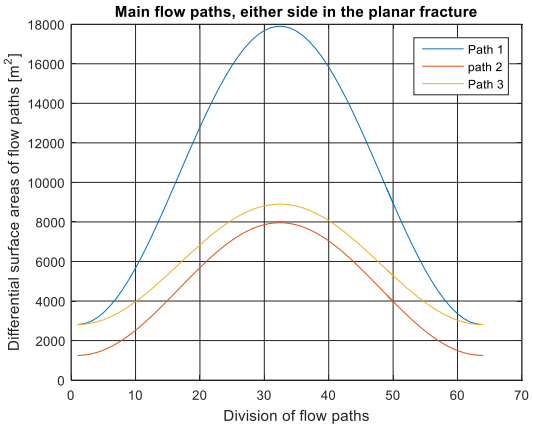

Figure 18: The surface area of each pixel along the flow path.

4.2 Numerical Simulation Results

Temperature fields, calculated from the numerical model along the flow paths of the coolant fluid for optimized distribution are shown in Fig. 19 for Cases 1 and 2 at three age, Years 1, 5 and 30 of the REGS reservoir. The rock wall as the interface supplies the thermal power from the hot rock strata through three-dimensional transient heat conduction to the coolant fluid. The thermal power as total heat flux exploited from the hot rock are calculated from the numerical model as a function of time, shown in Fig. 20 for Cases 1 and 2.

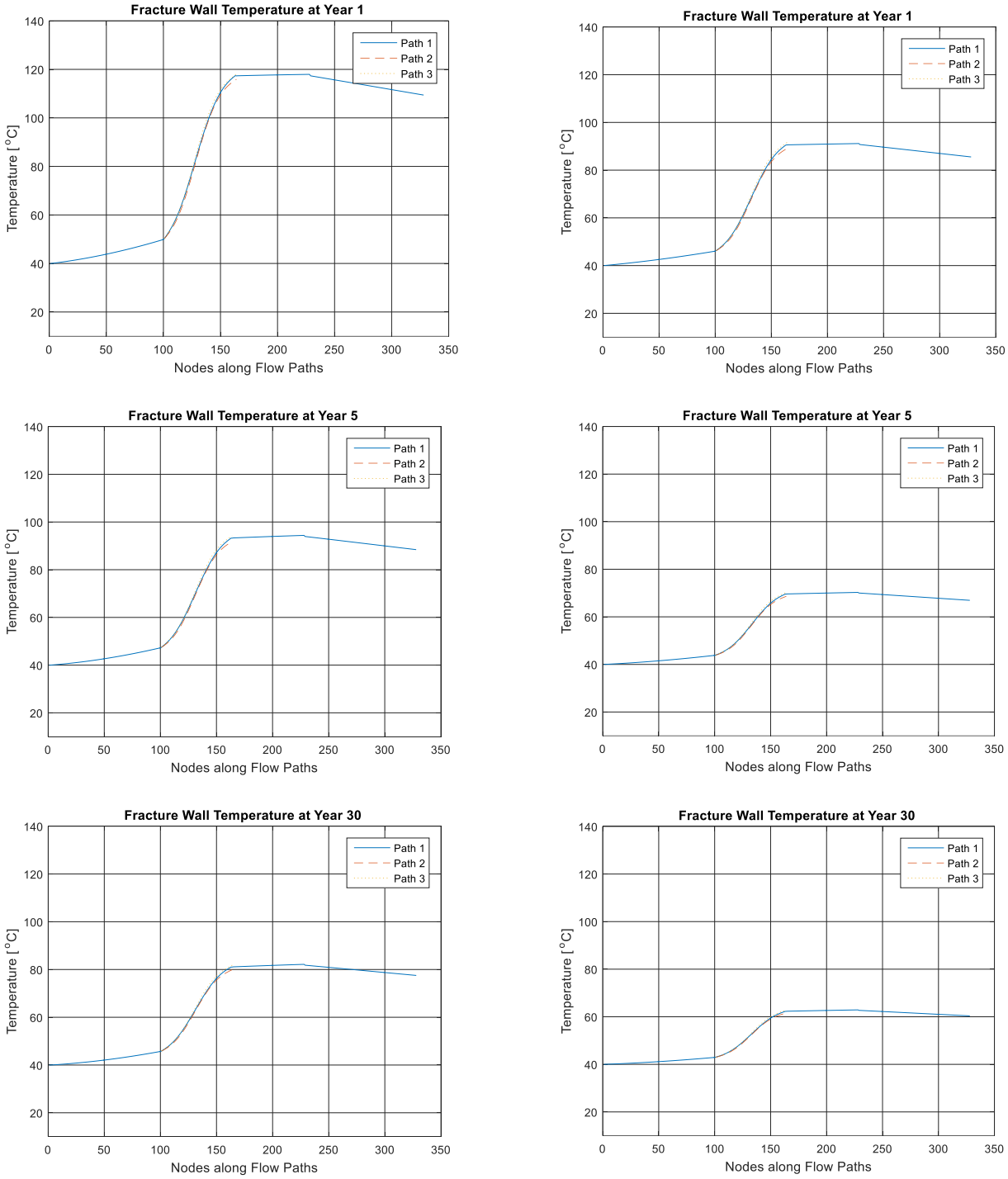

Figure 19: Temperature fields at Years 1, 5 and 30 for Case 1 (left) and Case 2 (right) for optimized fluid distribution between Path 1, 2 and 3.

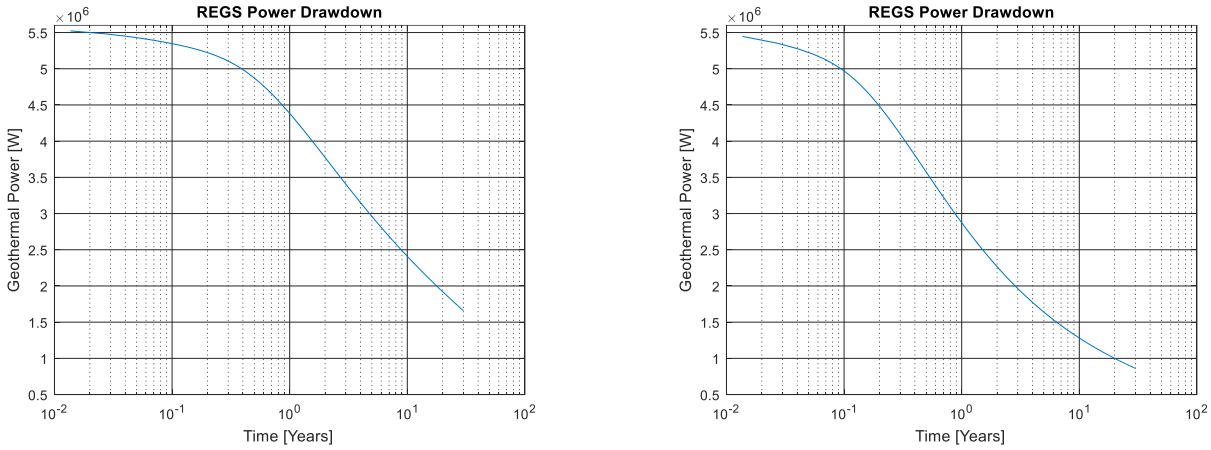

Figure 20: Thermal power drawdown for Case 1 (left) and Case 2 (right) for optimized fluid distribution between Path 1, 2 and 3.

The optimized fluid distribution of 47%, 28%, and 25% between Path 1, Path 2 and Path 3, respectively, provides near-identical exit temperatures at the end of the paths as shown in Figs. 19. For comparison and sensitivity check, the temperature filed is also modeled for a more realistic fluid distribution of 20%, 35%, and 45% between Path 1, Path 2 and Path 3, shown in Fig. 21 and Fig. 22 (as a continuation to Year 30). For this fluid distribution, the thermal power as total heat flux exploited from the hot rock is shown in Fig. 23 for Cases 1 and 2.

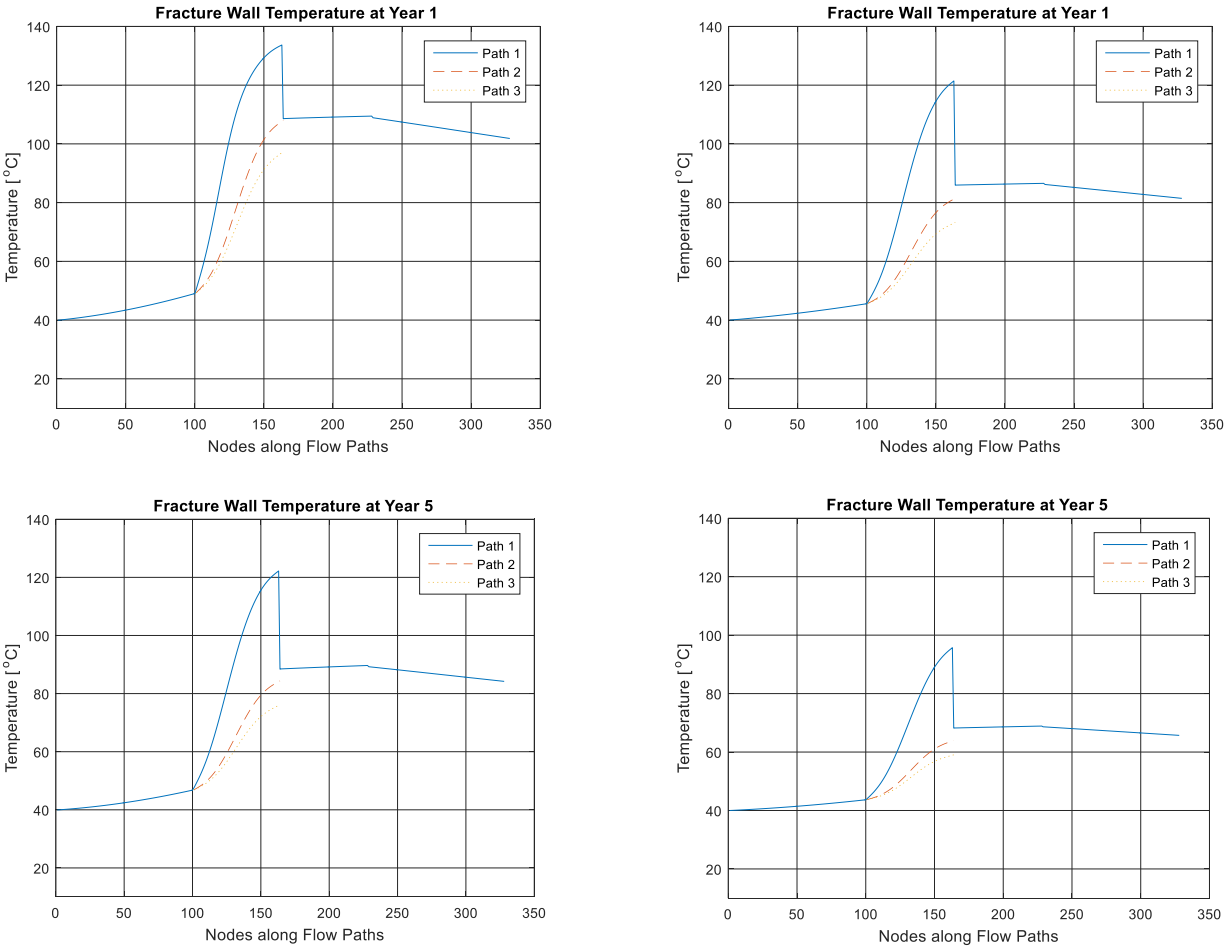

Figure 21: Temperature fields at Years 1 and 5 for Case 1 (left) and Case 2 (right) for a realistic fluid distribution between Path 1, 2 and 3.

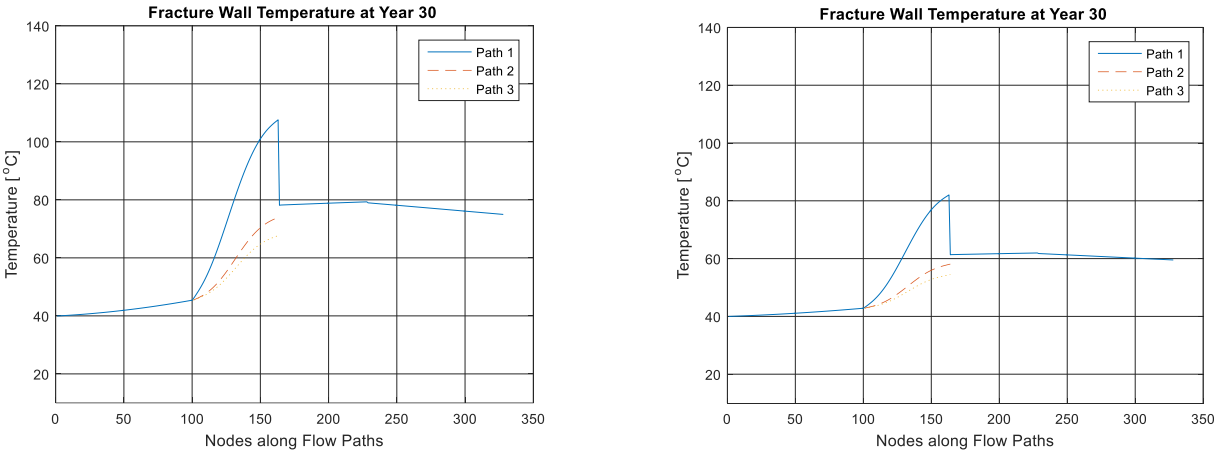

Figure 22: Temperature fields at Year 30 for Case 1 (left) and Case 2 (right) for a realistic fluid distribution between Path 1, 2 and 3.

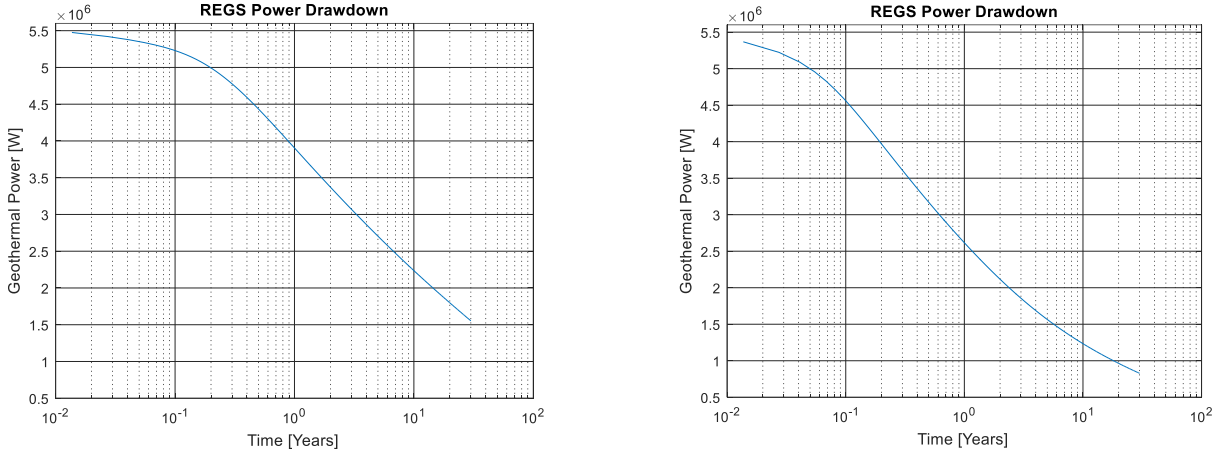

Figure 23: Thermal power drawdown for Case 1 (left) and Case 2 (right) for a realistic fluid distribution between Path 1, 2 and 3.

5. DISCUSSION OF ENERGY RECOVERY APPLICATION

The hydrofracturing technology for REGS assumes a crystalline base rock formation (such as granite) with high mass density and thermal conductivity. Case 1 represents such a formation. Case 2 differs from Case 1 only in the rock properties, representative to sedimentary formation, for comparison. Otherwise, the model setup, geometry and coolant flow are identical, resulting in similar characteristics in temperature distribution changing with space and time, albeit much lower production temperature and faster thermal drawdown in Case 2 than in Case 1.

The expected temperature distributions are shown in the left and right columns of Fig. 19, respectively, at Years 1, 5 and 30 for the rock-fluid interface at the wall for Case 1 and 2 for optimized fluid distribution in the planar fracture. It must be noted that the coolant fluid temperature distribution is found (but not shown for brevity) to be nearly identical with that of the rock wall due to a relatively high heat transport coefficient (and low thermal resistance) between the rock wall and the bulk temperature of the fluid at every node and time period. Therefore, Figs. 19 and 22 may be interpreted as the coolant fluid temperature variation as well with space and time.

The independent variable of the temperature variation is the node number starting along the injection well through nodes (1,100). Over these nodes, the rock wall and fluid temperature moderately increases due to the warming virgin rock temperature with depth and also amid the heat coming from the returning production pipe that runs upward in the well. The downward coolant flow continues in six parallel flow channels, three on the left and three on the right side of the symmetrical, planar fracture, illustrated in Fig. 14. The six parallel flow channels are represented by the parallel resultant of three flow paths, marked as Path 1, 2, and 3 through nodes (101, 164). These paths pick up the majority of the thermal energy, resulting in rapid temperature increase of the coolant fluid at the wall. The flow rate distribution between Paths 1, 2, and 3 greatly affect the rate of heat exchange as well as the temperature increase in the individual flow channels. As shown, the three temperatures are matched well by trial-and error, refining the mass flow split ratio during numerical simulations until the temperature differences were reduced to just enough to see three curves for illustration.

From node 164, all paths merge into the first section of the upward production pipe through nodes (165, 228) which are all in contact with the hot support island in the center of the fracture. The wall temperature and the coolant fluid slightly rises in spite of a declining virgin rock temperature with elevation, indicating a moderate gain of thermal energy especially at Years 5 and 30. The last section of the thermally-insulated production pipe runs through the center of the injection well for nodes (229,328). Parasite heat exchange due to convection and conduction takes place between the cold injection and hot production fluids, heating and cooling them, respectively, along this section. The temperature variation with increasing elevation decreases slightly for the wall of the inner tube, replacing the rock wall for this section in the model. The temperature decrease of the wall (and inner-tube fluid temperature) is only a few degree Celsius due to the parasite heat exchange. It worth accepting a small temperature loss for the benefit of using k=0.2 [W/(mK)], a moderately low thermal conductivity in the thermal insulation of the production pipe. Such a moderate thermal conductivity may be satisfied with the selection of a low-density, but still sturdy plastic coating material that can likely withstand the insertion of a 2,000-m long pipe section without suffering structural damage.

The expected temperature distributions for Case 1 and 2 for a realistic fluid distribution in the planar fracture are shown in the left and right columns, respectively, in Fig. 21 at Years 1, 5 and in Fig. 22 at Year 30 for the rock-fluid interface at the wall. Although the temperatures in Paths 1, 2 and 3 are very different from each other, it is interesting to observe that the temperature of the merged paths in the common flow section from node 165 is not much different from the temperatures obtained in the optimized fluid distribution case shown in Fig. 19. However, a slight difference may be noticed, favoring the optimized fluid distribution case. It is assumed that a more unfavorable, or extreme fluid distribution (such as closing entirely one path or two) would result in a rapid deterioration in the resultant production temperature. It is assuring to see, however, that the planar fracture flow system is quite tolerant to fluid distribution un-balances from that of the optimal case.

The thermal power drawdowns with time for Case 1 (granite) and Case 2 (sedimentary rock) are shown in the left and the right sides of Fig. 20, respectively, for optimized fluid distribution in the planar fracture. Cases 1 and 2 start with almost the same, higher than 5 MW thermal power at time zero. The power output at month 2 age is still around 5 MW in Case 1 but the output drops to 4 MW in Case 2. The Case 2 reservoir will more rapidly loose power with time than the Case 1 plant, showing the importance of site selection for higher rock density and thermal conductivity. Nevertheless, both Case 1 and Case 2 sites can produce significant power and energy over 30 years with an average rate of power output of 2.19 MW and 1.27 MW, respectively. The average power output values may be converted to average kWh thermal energy, giving 2,190*8,766=19,198 MWh and 1,270*8,766=11,133 MWh energy per year for Cases 1 and 2, respectively. Assuming $0.07/kWh energy cost saving from heating with geothermal energy instead of electrical energy, the gross cost savings from electrical energy replacement are $40.3M and $23.4M, by applying a Case 1 or Case 2 REGS reservoir, respectively, for 30 years.

Considering that the active, total surface area of the planar fracture in the example is 565,487 m^2, the harvested power flux densities at Year 30 are 1,600,000/365,487=2.82 W/m^2 and 800,000/365,487=1.41 W/m^2. These values are still well over the natural, geothermal power flux density determined by the thermal conductivity and the geothermal gradient as q_1=3.5*0.05=0.175 W/m^2 and q_2=1.28*0.05=0.064 W/m^2 for Cases 1 and 2, respectively. The “collection factor,” definable as the ratio, are 2.82/0.175=16.11 and 1.41/0.064=22.033 for Cases 1 and 2, respectively.

It is interesting to see a decreasing rate of decline in Case 2 at longer time period: an extrapolation to 100 years indicates power output still over 0.5 MW (0.88 W/m^2), about 13.75 times the natural geothermal power flux density of 0.064 W/m^2.

Finally, a low sensitivity to the fluid flow distribution ratio between Paths 1, 2, and 3, is seen by comparing the power drawdowns in Figs. 20 and 23. The difference between them is a slightly favorable power output for the ‘optimized’ over the ‘realistic’ flow distribution in either a Case 1 or Case 2 reservoir.

6. CONCLUSIONS AND RECOMMENDATIONS

Test preliminary results for technology elements of a proposed, new EGS arrangement (called REGS) is presented. Such tests must continue to uncover and solve uncertainties in the REGS in order to bring the risk levels below the known risks of the currently considered and published EGS systems.

The geothermal energy extraction efficiency of the new REGS is studied for two cases in a boldly simplified arrangement in order to support the feasibility considerations for field tests. The arrangement requires only a single well and a 600 m diameter planar wing fracture created from the well.

Numerical simulations show that an average, gross thermal power output of 2.19 MW and 1.27 MW may be harvested from a Case 1 and Case 2 type rock around the REGS reservoir, respectively, for a 30-year operation time period. The gross market value of the geothermal energy that can be harvested form a Case 1 and Case 2 REGS-type reservoir are $40.3M and $23.4M, respective, counted at $0.07/kWh rate of energy cost.

The numerical simulation shows little temperature loss and thus sensitivity to parasite heat exchange through the thermal insulation of the pipe-in-pipe fluid flow system in the single-well arrangement.

As an overall conclusion and recommendation, a REGS reservoir in either a Case 1 or Case 2 rock formation can be quite advantageous in view of its simplicity and economic potential, two factors in support for a field test in one of the existing, available, deep, dry holes in an exploited oil field.

7. ACKNOWLEDGEMENTS

The research was carried out with the support of the GINOP-2.3.2-15-2016- 00010 “Development of enhanced engineering methods with the aim at utilization of subterranean energy resources” project of the Research Institute of Applied Earth Sciences of the University of Miskolc in the framework of the Széchenyi 2020 Plan, funded by the European Union, co-financed by the European Structural and Investment Funds

REFERENCES

Bahrami, D., Danko, G., and Vazquez, R.: Fracture and Flow System Modeling Method for an EGS Reservoir. *Proceedings,* Thirty-Eighth Workshop on Geothermal Reservoir Engineering, Stanford University, Stanford, California, February 21, (2016). p. 1-12.

Cornet, F.H.: In-situ Determination Techniques and Their Robustness. *GRC Workshop*, Sacramento, CA, (2016).

Danko, G.: MULTIFLUX V5.0 Software Documentation Qualification Documents, Software Tracking Number: 1002-5.0-00, *Software Management Office, Berkeley National Laboratory*. (2008), 1-1002

Danko, G., Bahrami, D., Varga, G., Baracza, M.K., and Jobbik, A.: Conceptual Study of a Well-Fracture-Well Type Fluid Circulation System for EGS. *PROCEEDINGS, 44th Workshop on Geothermal Reservoir Engineering*, Stanford University, Stanford, California, February 12-14, (2018). SPG-TR-213 p. 1-9.

DOE (Department of Energy): History of Geothermal Energy Research and Development in the United States, Reservoir Engineering 1978-2006. *Geothermal Technology Program*, (2006), 59-61.

Hermida, A.: Deflection and Stress in Preloaded Square Membrane. *GSC-13367*, Vol. 15, No. 9, (1991). p. 96.

Kumar, D., and Ghassemi, A.: Hydraulic Stimulation of Multiple Horizontal Wells for EGS Reservoir Creation. *GRC Proceedings*, Sacramento, CA, (2016) p. 373-381.

Jung, R.: EGS–goodbye or back to the future. *Effective and Sustainable Hydraulic Fracturing*, (2013), 95–121,

UNR, US patent disclosure: (WIPO) Systems and Methods for Enhancing Energy Extraction from Geothermal Wells. *International Publication* WO/2017/173329 A1 (PCT/US2017/025473) (2018), 1-17.

Zhou, M., Cho, J., Zerpa, L., and Augustine, C.: Optimization of Well in a Sedimentary Enhanced Geothermal Reservoir. *GRC Proceedings,* Sacramento, CA, (2016). p. 383-394.